Supplementary Material

Adsorptive Fractionation of Extracellular Polymeric Substances on Iron Oxyhydroxides: Impact on Copper Binding

Dan Luo [a,b,#], Sipei Yang [a,b,#], Haoyang Wang [a,b], Zhibin Wu [a,b], Xiaomin Gong [a,b], Yuan Yang[a,b], Yunshan Liang [a,b*], Yaoyu Zhou [a,b]

[a] Hunan Provincial Key Laboratory of Rural Ecosystem Health in Dongting Lake Area, College of Environment and Ecology, Hunan Agricultural University, Changsha, Hunan 410128, China

[b] Yuelushan Laboratory, Hongqi Road, Changsha, Hunan 410128, China

*Corresponding authors at: College of Environment and Ecology, Hunan Agricultural University, Changsha 410128, PR China

E-mail addresses: liang-123@hunau.edu.cn (Y. Liang).

Author Contributions D.L. and S.Y. contributed equally.

List of Figures

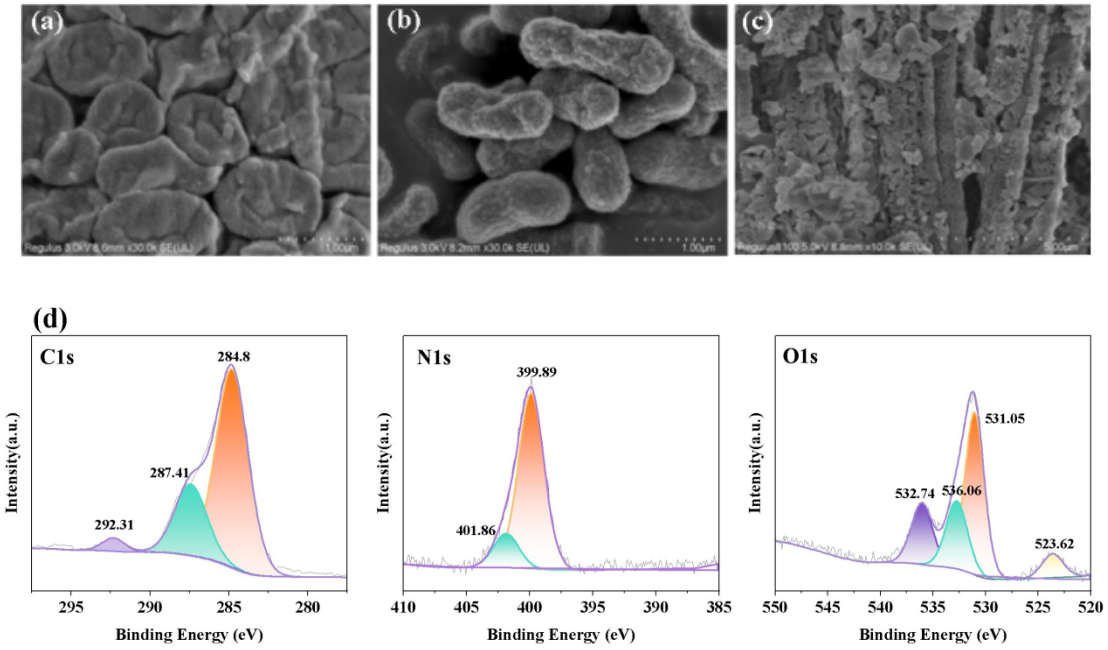

Fig. S1. Scanning electron microscope (SEM) images of *B. subtilis* before and after the removal of EPS (a) (b), along with SEM images and XPS high resolution spectra of the extracted EPS (c) (d).

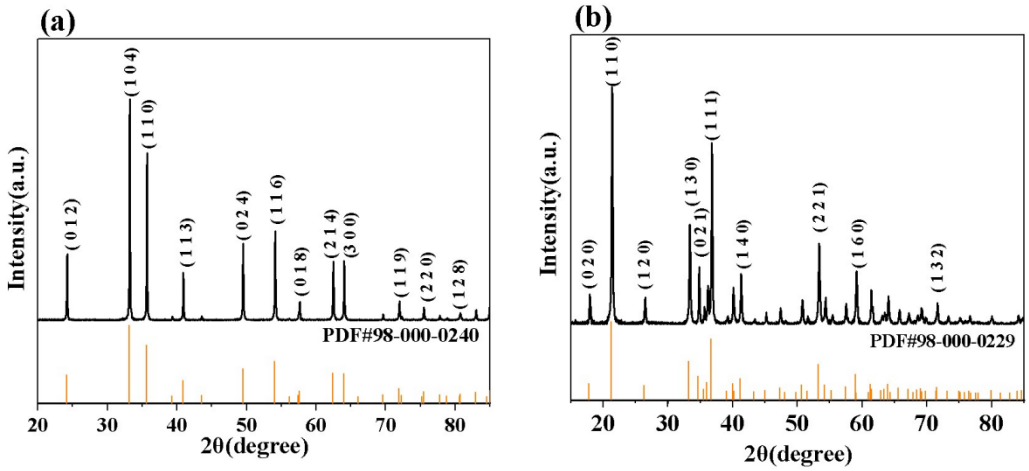

Fig. S2.XRD diffractograms of (a) Hema and Goet.

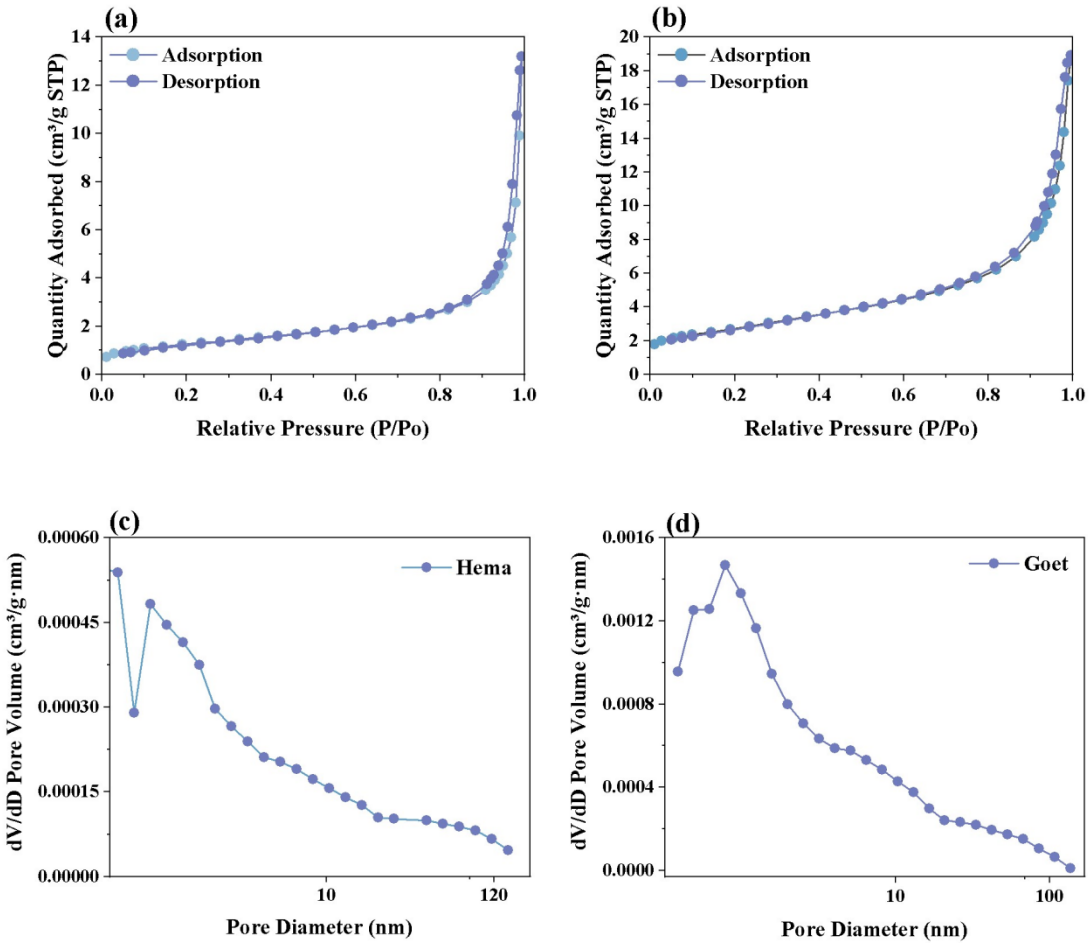

Fig. S3. Nitrogen adsorption isotherms at 77 K and BJH pore size distributions of Hema (a, c), Goet (b, d).

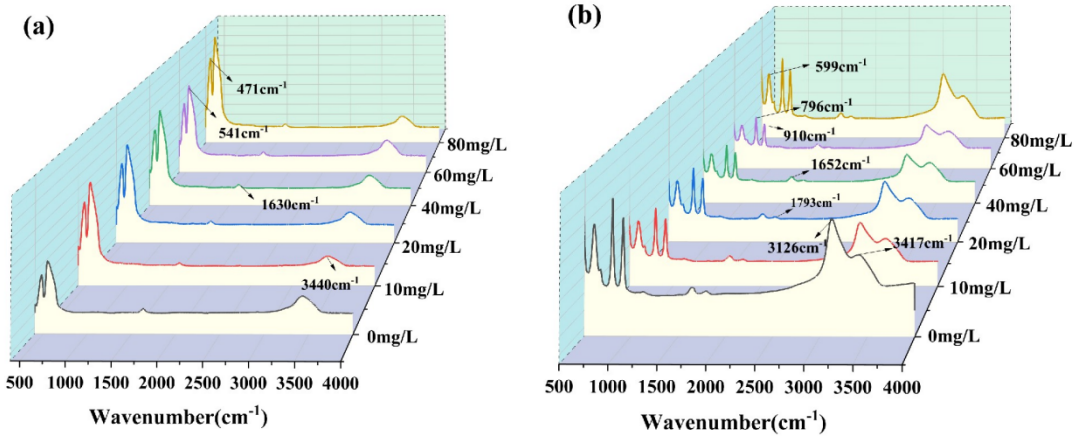

Fig. S4. FTIR spectra of Hema (a) and Goet (b) before and after EPS adsorption.

Fig. S5. 3D-EEM change of original EPS and EPS after equilibrium reaction with Hema and Goet where the sequence of #1~#5 shows the gradual increase of initial EPS concentration (10~80 mg C/L). H is represented Hema, G is represented Goet (background electrolyte was 0.01 M NaCl, temperature was 25 ± 1 ℃ and pH was ~7.0).

Fig. S6. Loading plots of the four fluorescent components of EPS before and after adsorptive fractionation on mineral surfaces.

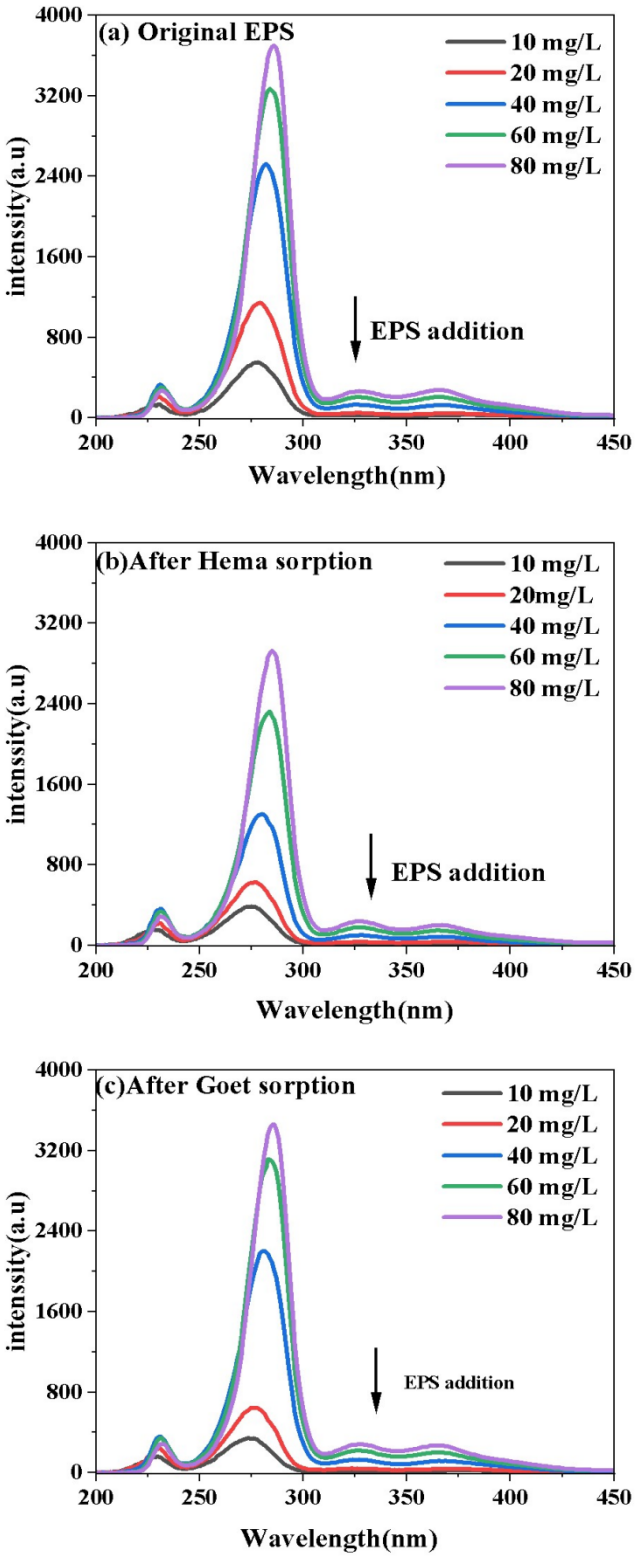

Fig. S7. Synchronous fluorescence spectra of EPS: (a) without mineral adsorptive fractionation; (b) after adsorptive fractionation on Hema; (c) after adsorptive fractionation on Goet.

Fig. S8. Loading plots of the four fluorescent components of EPS binding to Cu before and after adsorptive fractionation on mineral surfaces.

List of Tables

Table S1. Surface characteristics of iron oxyhydroxides.

	Specific Surface Area (m^2/g)	Pore Volume (cm^3/g)	Pore Size (nm)
Hema	4.5165 m^2/g	0.000337 cm^3/g	18.0758 nm
Goet	9.6892 m^2/g	0.000102 cm^3/g	12.0826 nm

* The Brunauer–Emmett–Teller (BET) equation was used to calculate surface areas from the nitrogen isotherm data. Barrett, Barrett, Joyner, Halenda (BJH) theory was used to obtain mesopore (pore diameter 1.7–300 nm) distributions from the desorption branch of the nitrogen isotherm. BJH cumulative and differential pore volume distributions were determined for the desorption branch of the isotherm. (Fig. S3)

Table S2. PARAFAC components and their comparison to other studies.

Component	Excitation wavelength (nm)	Emission wavelength (nm)	Interpretation	Literature
C1	225/285	340	Tryptophan-like, protein-like	C5[(1)]
C2	220/275	340	Tryptophan-like, protein-like	C1[(2)]
C3	225/280	305	Tyrosine-like, protein-like,	C1[(3)]
C4	320	425	Marine/ microbial humic-like	C2[(4)]

Table S3. 2D-SF-COS results on the assignment and sign of each cross-peak in a synchronous map of EPS.

	Position (v1/v2 nm)	Sign 230	280	328	365	Assignment of EPS
EPS-Hema	230	+				Tyrosine
	280	+(-)	+			Tryptophan
	328	+(-)	+(-)	+		Fulvic-like
	365	+(-)	+(-)	+(-)	+	Fulvic-like
EPS-Goet	230	+				Tyrosine
	280	+(-)	+			Tryptophan
	328	+(-)	+(-)	+		Fulvic-like
	365	+(-)	+(-)	+(-)	+	Fulvic-like

Table S4. PARAFAC components and their comparison to other studies.

Component	Excitation wavelength (nm)	Emission wavelength (nm)	Interpretation	Literature
C1	220/275	340	Tryptophan-like, protein-like	C1[5]
C2	225/275	305	Tyrosine-like, protein-like	C7[6]
C3	220/310	290/370	Marine/ microbial humic-like	C4[7]
C4	270/355	310/435	Fulvic acid-like component	C3[8]

Table S5. Cross-peak signs in the SF synchronous and asynchronous (in parentheses) maps of EPS fractions with Cu addition.

	Position (v1/v2 nm)	Sign 230	280	328	Assignment of EPS
EPS-Cu	230	+			Tyrosine
	280	+	+		Tryptophan
	328	+(-)	+(-)	+	Fulvic-like
EPS-Hema-Cu	230	+			Tyrosine
	280	+(-)	+		Tryptophan
	328	+(-)	+(-)	+	Fulvic-like
EPS-Goet-Cu	230	+			Tyrosine
	280	+	+		Tryptophan
	328	+(-)	+(-)	+	Fulvic-like

Table S6. Cross-peak signs in the FTIR synchronous and asynchronous (in parentheses) maps of EPS with Cu addition.

	Sites(cm^{-1})	Assignment	Signs					References
			620	1052	1400	1620	1706	
EPS-Cu	620	ring vibrations from aromatic amino acids and nucleotides	+					(9)
	1052	vibrations from the C-O-C rings and stretches of the P=O bond in the phosphate group from polysaccharide	+	+				(10)
	1400	COO^- stretches associated with amino acid	+	+	+			(11)
	1620	C＝O extension of the amide I band	+(-)	+(-)	+(-)	+		(11)
	1706	C=O stretching vibration of free carboxylic groups	+	+	+(-)	+	+	(12)

	Sites(cm^{-1})	Assignment	Signs				References
			982	1070	1400	1620	
EPS-Hema-Cu	982	O-P-O stretches associated with nucleic acids	+				(13)
	1070	C-O-C ring vibrations and C-OH stretches derived from polysaccharides	+(-)	+			(10)
	1400	COO^- stretches associated with amino acid	+(-)	+	+		(11)
	1620	C＝O extension of the amide I band	+(-)	+(-)	+(-)	+	(11)
	Sites(cm^{-1})	Assignment	Signs				References
			620	1052	1425	1620	
	620	ring vibrations from aromatic amino acids and nucleotides	+				(9)

	1052	vibrations from the C-O-C rings and stretches of the P=O bond in the phosphate group from polysaccharides	+	+			(10)
	1425	COO^- stretches associated with amino acid	+(-)	+(-)	+		(11)
	1620	C＝O extension of the amide I band	+	+(-)	+	+	(11)

References

1. Sit I, Young MA, Kubicki JD, Grassian VH. Distinguishing different surface interactions for nucleotides adsorbed onto hematite and goethite particle surfaces through ATR-FTIR spectroscopy and DFT calculations. Physical Chemistry Chemical Physics. 2023;25(30):20557-66.
2. Cohen E, Levy GJ, Borisover M. Fluorescent components of organic matter in wastewater: Efficacy and selectivity of the water treatment. Water Res. 2014;55:323-34.
3. Garaba SP, Albinus M, Bonthond G, Flöder S, Miranda MLM, Rohde S, et al. Bio-optical properties of the cyanobacterium Nodularia spumigena. Earth Syst Sci Data. 2023;15(9):4163-79.
4. Liu C, Shen Q, Gu X, Zhang L, Han C, Wang Z. Burial or mineralization: Origins and fates of organic matter in the water–suspended particulate matter–sediment of macrophyte- and algae-dominated areas in Lake Taihu. Water Res. 2023;243.
5. Nimptsch J, Woelfl S, Osorio S, Valenzuela J, Ebersbach P, von Tuempling W, et al. Tracing dissolved organic matter (DOM) from land-based aquaculture systems in North Patagonian streams. Sci Total Environ. 2015;537:129-38.
6. Murphy KR, Hambly A, Singh S, Henderson RK, Baker A, Stuetz R, et al. Organic Matter Fluorescence in Municipal Water Recycling Schemes: Toward a Unified PARAFAC Model. Environ Sci Technol. 2011;45(7):2909-16.
7. Zhou X, Johnston SE, Bogard MJ. Organic matter cycling in a model restored wetland receiving complex effluent. Biogeochemistry. 2022;162(2):237-55.
8. Wang H, Wang Y, Zhuang WE, Chen W, Shi W, Zhu Z, et al. Effects of fish culture on particulate organic matter in a reservoir-type river as revealed by absorption spectroscopy and fluorescence EEM-PARAFAC. Chemosphere. 2020;239.
9. He C, He X, Yuan R, Li N, Jiang J. Binding characteristics of Pb and Zn to low-temperature feces-based biochar-derived DOM revealed by EEM-PARAFAC combined with general and moving-window two-dimensional correlation analyses. Environ Sci Pollut Res. 2022;30(10):27525-38.
10. Zhu Y, Jin Y, Liu X, Miao T, Guan Q, Yang R, et al. Insight into interactions of heavy metals with livestock manure compost-derived dissolved organic matter using EEM-PARAFAC and 2D-FTIR-COS analyses. J Hazard Mater. 2021;420.
11. Hu B, Wang P, Wang C, Qian J, Bao T, Shi Y. Investigating spectroscopic and copper-binding characteristics of organic matter derived from sediments and suspended particles using EEM-PARAFAC combined with two-dimensional fluorescence/FTIR correlation analyses. Chemosphere. 2019;219:45-53.
12. Li X, Yang J, Chen C, Vähätalo AV, Riise G, Liu C, et al. Effects of mineral adsorption on the molecular composition of soil dissolved organic matter: Evidence from spectral analyses. Chem Geol. 2024;669.
13. Li K, Yang S, Wang H, Wu Z, Liang Y, Gong X, et al. Molecular spectra and docking simulations investigated the binding mechanisms of tetracycline onto E. coli extracellular polymeric substances. Talanta. 2024;276.